Valence-state and spin-state transition of Co in $LaCo_{0.5}Rh_{0.5}O_3$

S.-C. Liao,[1] S. C. Haw,[2,*] C. Y. Kuo,[1,2] H. Guo,[1] H. B. Vasili,[3] S. M. Valvidares,[3] A. C. Komarek,[1] H. Ishii,[2] S. A. Chen,[2] H. J. Lin,[2] A. Tanaka,[4] T. S. Chan,[2] L. H. Tjeng,[1] C. T. Chen,[2] Z. Hu,[1] and J. M. Chen[2,†]

[1]*Max Planck Institute for Chemical Physics of Solids, Nöthnitzer Strasse 40, 01187 Dresden, Germany*

[2]*National Synchrotron Radiation Research Center, 101 Hsin-Ann Road, Hsinchu 30076, Taiwan*

[3]*ALBA Synchrotron Light Source, E-08290 Cerdanyola del Vallès, Barcelona, Spain*

[4]*Department of Quantum Matter, ADSM, Hiroshima University, Higashi-Hiroshima 739-8526, Japan*

(Received 4 September 2018; revised manuscript received 9 January 2019; published 6 February 2019; corrected 11 November 2019)

We have observed that the Rh substitution for Co in $LaCo_{0.5}Rh_{0.5}O_3$ leads to the spectral feature at the Co-$L_{2,3}$ absorption edge taken at 300 K similar to that in $LaCoO_3$ taken at 650 K, in which the spin state of magnetic Co^{3+} ions has been controversially discussed in the past decades and can be easily clarified by studying $LaCo_{0.5}Rh_{0.5}O_3$ without worrying about oxygen loss induced at high temperature. Our combined experimental and theoretical x-ray absorption spectroscopy (XAS) at the Co-$L_{2,3}$ and the experimental Rh-$L_{2,3}$ edges indicated a nearly 1:1 mixture of high-spin (HS) and low-spin (LS) $Co^{3+}(3d^6)$ and a LS $Rh^{3+}(4d^6)$ in contrast to the Co^{2+}/Rh^{4+} state found in Ca_3CoRhO_6 at room temperature. Upon cooling only a small portion of the HS Co^{3+} ions was converted to a LS state until 10 K in $LaCo_{0.5}Rh_{0.5}O_3$. The Co-$K\beta$ x-ray emission spectra revealed a gradual spin-state transition from a mixed LS/HS at ambient pressure to a complete LS state of Co^{3+} ions up to 14 GPa. The theoretical and experimental intensity ratio $I(L_3)/I(L_2)$ on the Co-$L_{2,3}$ edges and a comparison between the difference spectrum of $K\beta$ x-ray emission of $LaCo_{0.5}Rh_{0.5}O_3$ taken at ambient pressure (AP) and 14 GPa and that of Sr_2CoRuO_6 taken at AP and 39.6 GPa exclude the intermediate spin state of Co^{3+} in $LaCo_{0.5}Rh_{0.5}O_3$.

DOI: 10.1103/PhysRevB.99.075110

I. INTRODUCTION

Among the transition metal ions, cobalt is intriguing since it possesses not only charge degree of freedom, but also spin-state degree of freedom [1,2]. For example, three spin states are possible for cobalt ions: a high-spin (HS) state ($S = 2$), a low-spin (LS) state ($S = 0$), and even an intermediate-spin (IS) state ($S = 1$) for Co^{3+} ions [1,3,4] and HS state ($S = 5/2$), LS state ($S = 1/2$), and IS state ($S = 3/2$) for Co^{4+} ions [5–7]. The large diversity of physical phenomena displayed, including metal-insulating transitions [8–10], superconductivity [11], large magnetoresistance [12], high thermoelectric power [13], and high-performance catalysts for energy storage applications [14,15] is closely related to both charge and spin degrees of freedom of cobalt ions. A well-known example is $LaCoO_3$, where the Co^{3+} ions have a nonmagnetic LS ground state and undergo a gradual transition with increasing temperature to magnetic ions accompanying the metal-insulator transition [16–18]. The nature of the spin state (IS or HS) of the magnetic ions, however, was heavily disputed in the literature for many decades and is still a vivid topic now [19–22]. In fact, the LS is the ground state for Co^{3+} ions with an octahedral coordination in whole $RCoO_3$ ($R =$ rare earth) system; the magnetic ions can only be thermally populated.

Recently, hybrid solid-state oxides between a $3d$ and $4d$ ($5d$) transition metal (TM) with unpaired electrons have raised increasing interest in the scientific community because of very high ordering temperature [23] and the unusual spin state of TM ions [24–28]. The HS ground state of Co^{3+} ions with octahedral coordination was stabilized in a three-dimensional double perovskite structure $A_2BB'O_6$ such as Sr_2CoRuO_6, Sr_2CoIrO_6, and in layered $A_2B_{0.5}B'_{0.5}O_4$ perovskites like $Sr_2Co_{0.5}Ir_{0.5}O_4$ [24–28]. It was observed that the valence state of Co ions in $RCoO_3(Ca_3Co_2O_6)$ and $SrCoO_3(Sr_2CoO_4)$ would decrease from 3+ to 2+ and from 4+ to 3+, respectively, if 50% of the Co ions were replaced by $4d$ ($5d$) TM ions which have a 4+ state in $RCoRuO_6$ and Ca_3CoRhO_6, and a 5+ state in Sr_2CoRuO_6, Sr_2CoIrO_6, and $Sr_2Co_{0.5}Ir_{0.5}O_4$ due to the charge balance requirement [24–27,29]. However, the valence state and the spin state of Co ions [30–36] as well as the magnetic properties [37,38] were controversially discussed in the case of Rh substitution for Co ions in $LaCo_{1-x}Rh_xO_3$.

In this work, the charge and spin states of Co(Rh) were studied using soft x-ray absorption at the Co(Rh)-$L_{2,3}$ edge and the spin-state transition of Co ions under high pressure was explored using the Co-$K\beta$ x-ray emission spectra of $LaCo_{0.5}Rh_{0.5}O_3$ (LCRO). We have observed that the Rh substitution for Co in $LaCo_{0.5}Rh_{0.5}O_3$ leads to a large percentage of HS Co ions below room temperature, while in the undoped $LaCoO_3$, ~50% of the HS Co ions are thermally populated at 650 K. Therefore it takes major advantage of the study of the spin state of magnetic Co^{3+} ions in $LaCo_{0.5}Rh_{0.5}O_3$ without worrying about oxygen loss at high temperature.

II. EXPERIMENT

The polycrystalline samples of $LaCo_{0.5}Rh_{0.5}O_3$ were synthesized by solid-state reaction [38]. The phase purity was

*Corresponding author: ho.kelman@nsrrc.org.tw
†Corresponding author: jmchen@nsrrc.org.tw

TABLE I. Structural parameters of $LaCo_{0.5}Rh_{0.5}O_3$ at 300 K determined from powder neutron diffraction [38] and $LaCoO_3$ at 300 K from powder x-ray scattering [39].

	$LaCo_{0.5}Rh_{0.5}O_3$ at 300 K	$LaCoO_3$ at 300 K
Space group	*Pbnm*	*I*2/*a*
a, *b*, *c* (Å)	5.5334(1), 5.53113(9), 7.8168(2)	5.3682(3), 5.4326(4), 7.6386(5)
α, β, γ	90, 90, 90	90, 90.9818(7), 90
V (Å^3)	239.240(8)	222.73(3)
La	4*c*	4*e*
x, *y*, *z*	0.5092(8), 0.4632(4), 0.25	0.25, 0.24911(1), 0
B(Å^2)	0.77(8)	0.18(2)
Co, Rh	4*b*	4*c*
x, *y*, *z*	0.5, 0.0, 0.0	0.75, 0.25, 0.25
B(Å^2)	0.54(9)	0.39 (3)
O1	4*c*	4*e*
x, *y*, *z*	0.418(1), 0.0088(7), 0.25	0.25, -0.2997(2), 0
B(Å^2)	0.9(1)	0.52(3)
O2	8*d*	8*f*
x, *y*, *z*	0.7926(9), 0.217(1), 0.0379(5)	0.0213 (1), 0.0360(1), 0.2287(2)
B(Å^2)	1.36(9)	0.65 (3)
(Co, Rh)-O (Å) × 6	2.006(1) × 2, 1.962(5) × 2, 2.038(5) × 2	1.9854(8) × 2, 1.9287(2) × 2, 1.9726(7) × 2

confirmed by both x-ray diffraction (XRD) and powder neutron diffraction (PND). The ac susceptibility measurements showed that the freezing temperature (T_f) shifts to higher temperatures with increasing frequency, indicating the Co/Rh disorder and a spin-glass magnetic property [38]. The Co-$L_{2,3}$ x-ray absorption spectroscopy (XAS) measurements were recorded at the BL11A beamline of the National Synchrotron Radiation Research Center (NSRRC) in Taiwan. Clean sample surfaces were obtained by cleaving pelletized samples *in situ* in an ultrahigh-vacuum chamber with a pressure in the 10^{-10} mbar range. The Co-$L_{2,3}$ XAS spectra were collected using the surface sensitive total electron yield mode (TEY) with an energy resolution of about 0.25 eV, and the extended x-ray absorption fine structure (EXAFS) at the Co-*K* edge was performed at the BL17C1 beamline of NSRRC by using the transmission mode. The Rh-L_3 XAS spectra were measured at BL16A beamline of NSRRC using the bulk sensitive fluorescence yield mode and the Rh-$L_{2,3}$ x-ray magnetic circular dichroism (XMCD) spectrum was measured at the BL29 Boreas beamline of the ALBA Synchrotron Facility in Spain. The XMCD spectrum was measured at 80 K and in a magnetic field of 6 T with a degree of circular polarization of 70%. The Co-$K\beta$ x-ray emission spectra were obtained at the Taiwan inelastic x-ray scattering BL12XU beamline at SPring-8 in Japan. A Mao-Bell diamond anvil cell with a Be gasket was used for the high-pressure experiment. Silicon oil was served as a medium to transmit pressure. The applied pressure in the diamond anvil cell was measured through the Raman line shift of ruby luminescence before and after each spectral collection. The Co-$K\beta$ x-ray emission spectra were collected at 90° from the incident x ray and analyzed with a spectrometer (Johann type) equipped with a spherically bent Ge(444) crystal (radius 1 m) arranged on a horizontal plane in a Rowland-circle geometry.

III. RESULTS AND DISCUSSION

A. Crystal structure of LCRO

The powder neutron diffraction pattern of LCRO [38] was refined by the Rietveld method using the FULLPROF software package. The obtained structure data are presented in Table I together with structure data of $LaCoO_3$ for comparison [39]. The crystal structure can be described by the orthorhombic space group *Pbnm*. The very weak (1 0 1) Bragg peak indicates that the Co and Rh ions are randomly distributed in the sample.

It was found previously that the lattice constants for the Rh content $x = 0.4$, 0.5, and 0.6 along three crystallographic directions all increase with increasing Rh content x [38] due to the larger Rh^{3+} ionic radius [40]. Our results are consistent with previous studies [31,37]. Especially, the crossover of a and b lattice parameters can also be observed at $x = 0.5$. We expect that the large cell volume of LCRO as compared with that of $LaCoO_3$ shown in Table I would lead to a large Co-O bond length, and in turn a weak crystal field interaction as is known in Sr_2CoIrO_6 [24] and Sr_2CoRuO_6 [25]. Therefore at room temperature there would be a relatively large content of magnetic Co^{3+} ions in LCRO. Radaelli and Cheong have studied the detailed Co-O bond length in $LaCoO_3$ as a function of temperature from 5 up to 1000 K by means of high-resolution neutron powder diffraction and discussed the relation between the Co^{3+} spin state and the Co-O bond length [41]. In order to determine the real Co-O bond length in LCRO at room temperature, here we have measured the element-selective Co-*K* EXAFS, which is the most useful experimental method considering the Co/Rh-disorder in LCRO.

The Co-*K* EXAFS data were analyzed by using the IFEFFIT program. The average Co-O distance in LCRO is 1.953(6) Å

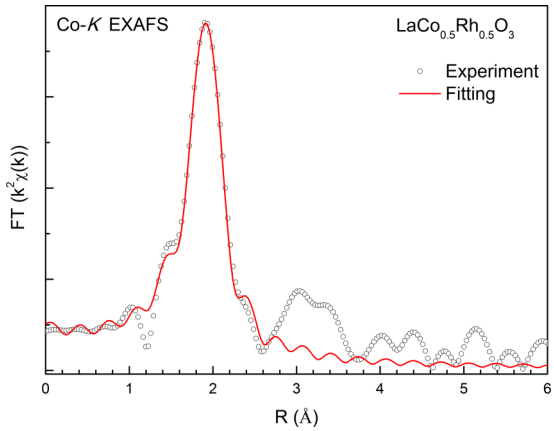

FIG. 1. Experimental (black circles) and simulated (red line) Fourier transforms of the k^2-weighted Co-K EXAFS data. Only the Co-O distances of the first coordination sphere were simulated.

obtained from the Fourier transforms of the k^2-weighted Co-K EXAFS data as shown in Fig. 1. This value is larger than the Co-O distance of 1.934 52(6) Å in $LaCoO_3$ at 300 K obtained from neutron diffraction [41], and larger than those of 1.925 Å [42], 1.932(1) Å [43], and 1.934 Å [44] obtained from Co-K EXAFS, but it is rather close to that of 1.952 79(7) Å in $LaCoO_3$ at 750 K [41]. In another disordered hybrid Co/Ir oxide, a much larger average Co-O distance of 1.967 Å was obtained from the Co-K EXAFS data giving rise to a pure HS Co^{3+} state [45]. The spin state of the magnetic Co^{3+} can be quite reliably determined by spectroscopic techniques. In case of $LaCoO_3$ about 20% of the HS Co^{3+} ions at room temperature was found previously [4]. From this consideration we performed more detailed spectroscopic studies on LCRO.

B. Experimental Co-$L_{2,3}$ XAS spectra

Considering Co^{2+}/Rh^{4+} and Co^{3+}/Ir^{5+} distribution in hybrid solid-state oxides Ca_3CoRhO_6 [29] and in $Sr_2Co_{0.5}Ir_{0.5}O_4$ [26,27], respectively, and the possible conversion of Co^{3+}/Rh^{3+} to Co^{2+}/Rh^{4+} suggested in [31], as well as mixed HS/IS in $LaCo_{1-x}Rh_xO_3$ [33], we first explore the detailed valence state and spin state of Co ions using the Co-$L_{2,3}$ XAS, although most works suggested Co^{3+} with mixed LS/HS spin state and LS Rh^{3+} state distribution [32–35].

Figure 2 shows the Co-$L_{2,3}$ XAS spectra of (a) LCRO taken at 300 K (red line) and 15 K (black line), (c) $Li_2Co_2O_4$ (LCO, blue line) as a LS Co^{3+} [46], Sr_2CoRuO_6 (SCRO, green line) as a HS Co^{3+} [25], and (d) CoO as a Co^{2+} reference. The spectral weight center of the L_3 white line shifts to higher energies as the valence of the cobalt ion increases: from Co^{2+} reference CoO to Co^{3+} reference LCO and SCRO. This reflects that x-ray absorption spectra at the transition-metal L_3 edge are highly sensitive to the valence state [25,29,47]. The "center of gravity" of the L_3 white line of LCRO lies about 2 eV higher in energy than that of CoO and at the same energy as those of Co^{3+} references LCO and SCRO indicating a Co^{3+} state.

Here we want to emphasize that the Co-L_3 edge is extremely sensitive to Co^{2+} content [25,48] as compared with

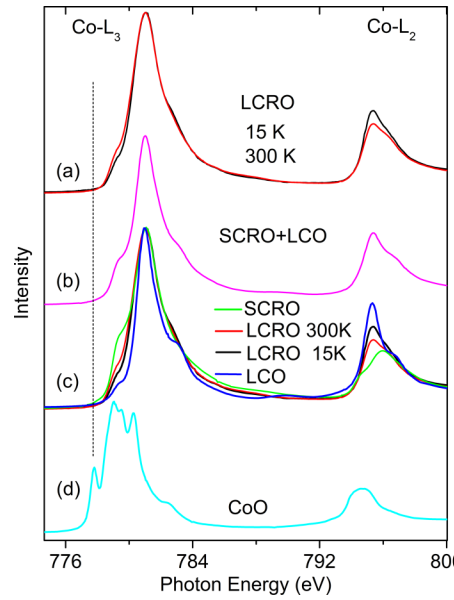

FIG. 2. The Co-$L_{2,3}$ absorption spectra of (a) LCRO taken at 300 K (red line) and 15 K (black line), (b) 1:1 sum of LCO and SCRO, (c) LCO (blue line) as a LS Co^{3+}, SCRO (green line) as a HS Co^{3+}, and (d) CoO (cyan line) as a HS Co^{2+} reference.

the Co-L_2 edge, since a sharp lowest-energy peak at 777.8 eV from the Co^{2+} ion is located outside the spectral features of Co^{3+} at the Co-L_3 edge, and it is a fingerprint of HS Co^{2+} with an octahedral local symmetry [25,48], while the Co-L_2 edge of Co^{2+} exhibits a broad and structure-loss spectral feature as shown in the bottom of Fig. 2. It was found previously that the sizable spectral intensity of the Co^{2+} state was observed in electron-doped $La_{0.7}Ce_{0.3}CoO_3$ at the Co-L_3 edge, but the Co^{2+} signal could not be detected at the Co-L_2 edge; therefore the Co-L_2 is not sensitive to Co^{2+} content and the possible partial conversion of Co^{3+}/Rh^{3+} to Co^{2+}/Rh^{4+} cannot be excluded from the Co-L_2 spectrum [32]. The lack of a spectral feature at 777.8 eV (see vertical dashed line) clearly indicates the absence of a Co^{2+} impurity, in other words a pure Co^{3+} state in our LCRO sample. In Fig. 2(c) we also present the LCRO spectrum taken at 300 K (red line) and 15 K (black line) for comparison. One can clearly see that the LCRO spectrum looks like a mixture of the LCO spectrum and the SCRO spectrum. As shown in Fig. 2(b), the spectrum (magenta line) obtained from a 1:1 mixture of the LCO spectrum and the SCRO spectrum is very similar to the LCRO spectrum taken at 300 K. This is different from $LaCoO_3$ with a LS ground state below 20 K [4], a 1:1 mixture of LS and HS Co^{3+} ions was found above 650 K [4]. Considering that soft x-ray spectroscopic measurements such as the Co-$L_{2,3}$ XAS and XPS are performed under ultrahigh-vacuum condition, heating the sample might lead to the oxygen loss at the sample surface. Therefore, the result of the spin state of magnetic Co^{3+} ions obtained from the experimental methods in LCRO is very reliable as compared with that in $LaCoO_3$.

C. Theoretical simulation on the Co-$L_{2,3}$ XAS spectra

Having ascertained the pure Co^{3+} valence state in LCRO, we now focus on the determination of the spin state of

Co^{3+} ions in LCRO. In this context, it is important to note that the multiplet structure of the x-ray absorption spectrum depends strongly on the valence, the orbital, and the spin states. Despite having the same Co^{3+} valence, the line shapes at both Co-L_3 and -L_2 edges are very different between LS Co^{3+} LCO and HS Co^{3+} SCRO in Fig. 2(c). Hence, the spectral line shape at both the Co-L_3 and -L_2 edges can be used as a fingerprint to determine the spin state. Although the Co-L_2 edge is also sensitive to the spin state of the Co^{3+} ion, to understand the magnetic property and obtain an accurate number of populated HS Co^{3+} ions, one has to study both the Co-L_3 and Co-L_2 edges for guaranteeing that the magnetic ions are only from HS Co^{3+} ions, but not Co^{2+} impurity.

In order to obtain the precise HS Co^{3+} content, we performed a quantitative analysis of the Co-$L_{2,3}$ spectra by using the well-proven configuration-interaction cluster model that includes the full atomic multiplet interaction, and the crystal field interaction, as well as the hybridization between the Co $3d$ and oxygen $2p$ according to Harrison's prescription [25–27]. The calculations were performed using the XTLS code [49]. In the calculation, we have considered three configurations for the wave function in the ground state: $\Psi_g = \alpha|3d^6\rangle + \beta|3d^7\underline{L}\rangle + \gamma|3d^8\underline{L}^2\rangle$(where $\underline{L}$ stands for ligand hole). The charge-transfer energy is given by $E(d^7\underline{L}) - E(d^6) = 2\,\text{eV}$, $pd\sigma = 1.7\,\text{eV}$, the d-d Coulomb repulsion $U_{dd} = 5.5\,\text{eV}$, and the $2p$-$3d$ Coulomb interaction by $U_{pd} = 7.0\,\text{eV}$; the Slater integrals have been reduced to 80% of their Hartree-Fock value; the ionic part of the crystal field $10Dq_{\text{ionic}} = 0.5\,\text{eV}$ for HS and $10Dq_{\text{ionic}} = 0.8\,\text{eV}$ for LS. The theoretical spectra were broadened with Lorentzian broadening of 0.5 eV for core hole lifetime [50–52] convoluted with Gaussian broadening of 0.4 eV for the band formation [21,53] considering sharp multiplet lines of $3d$ transition metal cations without any band effects [54]. The result was convoluted with 0.3 eV of Gaussian broadening for monochromator resolution at 780 eV.

Our theoretical spectra with 0.5:0.5 and 0.7:0.3 LS to HS ratio plotted in Fig. 3(b) nicely reproduce all features of the experimental Co-$L_{2,3}$ XAS spectra of LCRO taken at 300 and 15 K in Fig. 3(a), respectively, further demonstrating the mixed LS-HS Co^{3+} ground state in this system. In Figs. 3(c) and 3(d), we also present calculated IS(1) ($d_{x^2-y^2}\underline{d_{xy}}$) and IS(2) ($d_{z^2}\underline{d_{xy}}$) spectra, respectively. Here, the underline denotes a hole and z^2 is an abbreviation of $3z^2$-r^2. One can see clearly that both IS spectra are very different from experimental LCRO spectra especially at the Co-L_2 edge, where theoretical line shapes of the IS state cannot be reproduced by the sum of LS and HS as shown in Fig. 3(e).

Another important point is that IS(1) and IS(2) spectra have $I(L_3)/I(L_2)$ ratios of 2.17 and 2.20, respectively, which are much smaller than 2.42(2.5) for LS and 3.54(3.64) for HS in calculated (experimental) spectra and therefore smaller than the experimental spectrum of LCRO at 300 K and 2.98 calculated for 1:1 mixed LS Co^{3+} and HS Co^{3+}.

Therefore, the mixed LS-HS in our theory can well reproduce experimental LCRO spectra at 15 and 300 K, while the calculated IS spectra have a different line shape from the experimental spectra of LCRO and have $I(L_3)/I(L_2)$ ratios much smaller than those of the experimental spectra of LCRO.

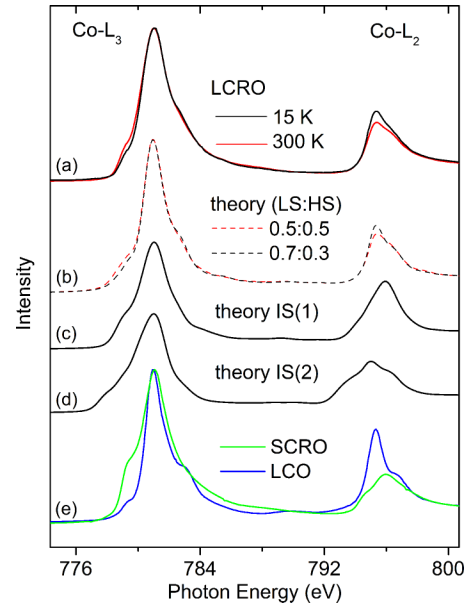

FIG. 3. The Co-$L_{2,3}$ absorption spectra of (a) LCRO taken at 300 K (red line) and 15 K (black line), (b) the theoretical 0.5:0.5 (red dotted line) and 0.7: 0.3 (black dotted line) ratio of LS:HS spectra, (c) theoretical IS(1) ($d_{x^2-y^2}\underline{d_{xy}}$) (black line) and (d) IS(2) ($d_{z^2}\underline{d_{xy}}$) spectra (black line), and (e) LCO (blue line) as a LS-Co^{3+} reference and SCRO (green line) as a HS-Co^{3+} reference.

The IS Co^{3+} is the Jahn-Teller ion and is expected to be stabilized under the following condition: a strong tetragonal distortion together with a very short in-plane Co-O distance [26,28]. Band formation has been proposed to possibly provide another route for the stabilization of IS Co^{3+} [55,56]. Although the IS is about 200 [4] to 400 meV [57] above the HS in $RCoO_3$ systems, both HS and IS have a band dispersion about 400 meV [21] therefore one cannot exclude a possible mixing between IS and HS.

D. Experimental Rh-L_3 XAS spectra

Having determined a Co^{3+} with a mixed spin state in LCRO, we turn to the Rh-L_3 edge to further confirm the Rh^{3+} state as expected for charge balance requirement, while the spin state of Rh^{3+} ions is generally expected to be in a LS state for $LaCo_{0.5}Rh_{0.5}O_3$ [31,36–38,58].

Figure 4 shows the XAS spectra at the Rh-L_3 edge of LCRO (blue line) and Ca_3CoRhO_6 (red line) as a Rh^{4+} reference [30]. The Rh-L_3 spectrum shows a single symmetry peak at the Rh-L_3 edge of LCRO, while an additional low-energy shoulder is observed for Ca_3CoRhO_6. The peak position in the LCRO spectrum is shifted by 1.5 eV to lower energies compared to that of the Ca_3CoRhO_6 indicating that the Rh valence state decreases from Rh^{4+} in the latter to Rh^{3+} in the former fulfilling the charge balance requirement for the Co^{3+}/Rh^{3+} valence state [29].

Furthermore, the single-peaked spectral structure for LCRO indicates LS Rh^{3+} ($4d^6$) with completely filled t_{2g} orbitals, i.e., only the transitions from the $2p$ core levels to the e_g are possible. The lower-energy shoulder at the Rh-L_3 edge of Ca_3CoRhO_6 can be attributed to transitions from the

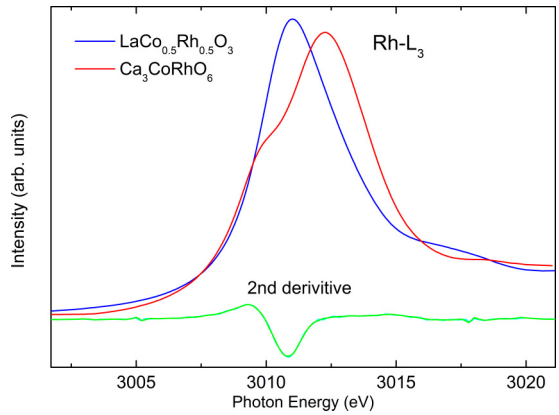

FIG. 4. Rh-L_3 XAS spectra of LCRO (blue line) together with Ca_3CoRhO_6 (red line) as a Rh^{4+} reference. The green line below the experimental data is the second derivative of LCRO.

$2p$ core levels to the t_{2g} state, reflecting a $4d^5$ configuration with one hole at the t_{2g} state. An undetected shoulder spectral feature in the second derivative spectrum [59] (green line) of LCRO clearly indicates that Rh is a nonmagnetic ion ($S = 0$); e.g., only Co ions contribute magnetism, since the t_{2g}-related spectral feature would be observed for IS($t_{2g}^5 e_g^1$) and HS($t_{2g}^4 e_g^2$) Rh^{3+} ions. To further confirm the LS Rh^{3+} state, we have measured the Rh-$L_{2,3}$ XMCD spectrum of LCRO which is presented in Fig. 5. The x-ray absorption spectra were measured with circularly polarized light with the photon spin parallel σ^+ (black line) and antiparallel σ^- (red line) aligned to the magnetic field. The difference spectrum, called XMCD (blue line), in Fig. 5 has no signal at both Rh-L_2 and Rh-L_3 edges supporting the LS ($S = 0$) state for Rh^{3+} ions in LCRO.

The mixed spin state of Co^{3+} means that the subtle balance between Hund's rule exchange interaction and crystal field interaction reaches a situation where LS and HS are nearly degenerated in LCRO even at room temperature. We expect that the mixed spin state Co^{3+} ion in LCRO can be easily converted to a pure LS state under external pressure as compared with the pure HS Co^{3+} ground state in SCRO [25] and $Sr_2Co_{0.5}Ir_{0.5}O_4$ (SCIO) [28].

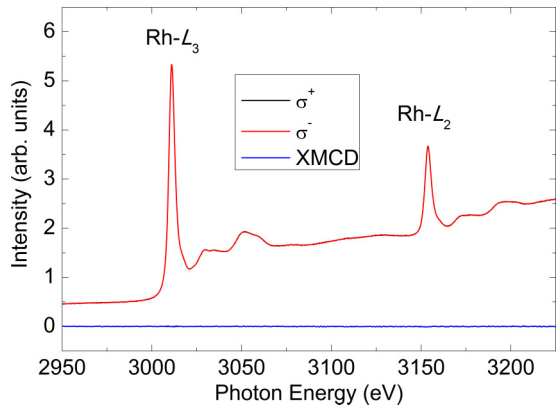

FIG. 5. The Rh-$L_{2,3}$ XMCD spectra of LCRO. The black and red lines represent the absorption spectra with photon spin parallel σ^+ and antiparallel σ^- aligned to the magnetic field, respectively. The blue line represents the XMCD.

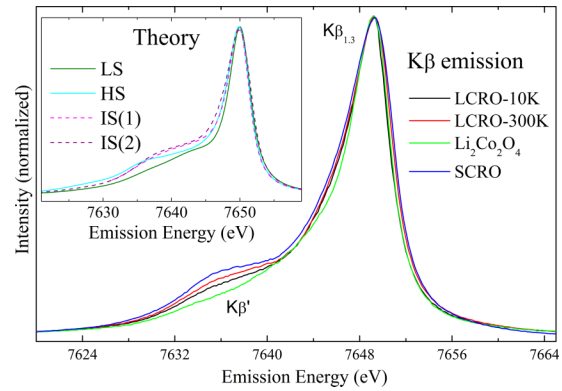

FIG. 6. The Co-$K\beta$ x-ray emission spectra (XES) of LCRO taken at 10 K (black line) and 300 K (red line) together with $Li_2Co_2O_4$ (green line) as a LS Co^{3+} reference and SCRO (blue line) as a HS Co^{3+} reference. The inset shows the theoretical Co-$K\beta$ XES spectra of HS (cyan line), LS (olive line), IS(1) ($d_{x^2-y^2}\underline{d_{xy}}$) (magenta dashed line), and IS(2) ($d_{z^2}\underline{d_{xy}}$) (purple dashed line) Co^{3+}.

E. Pressure-induced spin-state transition of Co^{3+}

To investigate whether the mixed HS-LS state in LCRO can be converted to a pure LS state upon applying pressure, we utilized the Co-$K\beta$ x-ray emission spectrum, which is well known to be sensitive to quantum number of the spin [25,28].

Figure 6 shows the Co-$K\beta$ x-ray emission spectra (XES) of LCRO taken at 10 and 300 K together with those of SCRO as a HS Co^{3+} reference and LCO as a LS Co^{3+} reference for comparison. The Co-$K\beta$ emission spectrum represents a main peak located at ~7650 eV corresponding to the $K\beta_{1,3}$ line and a pronounced satellite peak at ~7637 eV corresponding to the $K\beta'$ line. The intensity ratio of the low-energy $K\beta'$ line to the main emission $K\beta_{1,3}$ line is proportional to the number of unpaired electrons in the incomplete $3d$ shell [60] and can be used as an indicator of spin states in the material [25,28,60–62].

Although the intensity of the $K\beta'$ line decreases from 300 to 10 K for LCRO, the mixed spin state can be easily concluded since the spectral intensity of $K\beta'$ of LCRO at both 10 and 300 K locates between those of SCRO and LCO, which is in agreement with the results from the above Co-$L_{2,3}$ and the O-K XAS spectra [32].

Figure 7 shows the evolution of the Co-$K\beta$ emission line of LCRO as a function of pressure from ambient up to 31 GPa at room temperature. With increasing pressure, the intensity of the low-energy $K\beta'$ line decreases and almost disappears at 14 GPa and remains unchanged up to 31 GPa (Fig. 7). Such pressure-induced decrease of the spectral weight of $K\beta'$ line has been observed in $LaCoO_3$ [61], $BiCoO_3$ [63], SCRO [25], SCIO [28], and Sr_2CoO_5F [64].

Due to a relatively short Co-O distance $d_{Co-O} \sim 1.9345$ Å in $LaCoO_3$ at room temperature, the pressured-induced change of the $K\beta'$ spectrum is very weak [61]; therefore one cannot draw a conclusion from the $K\beta'$ spectrum as to whether IS is relevant or not in $LaCoO_3$. In $BiCoO_3$, the

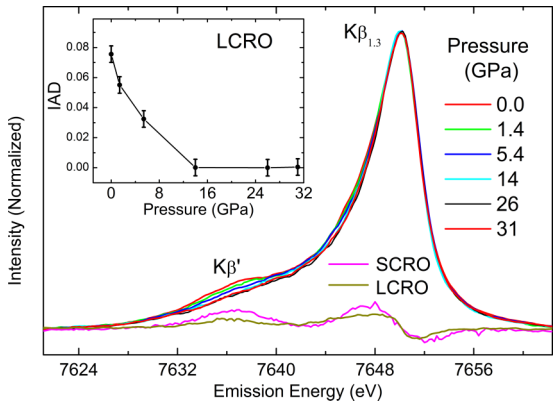

FIG. 7. Co-$K\beta$ x-ray emission spectra as a function of pressure and difference spectrum of Co-$K\beta$ emissions measured between ambient pressure (AP) and 14 GPa of LCRO (dark yellow line) and difference spectrum between AP and 40 GPa of SCRO (magenta line). Inset: integrated absolute difference (IAD) as a function of pressure for LCRO.

change from fivefold at atmospheric pressure to sixfold coordination above 3 GPa from a high-pressure structure study and HS to LS transition was expected. However, the high-pressure $K\beta'$ study indicated HS to IS transition and the reason for this discrepancy is not clear [63]. Indeed the spin-state transition of Co^{3+} from HS atmospheric pressure to LS at high 12 GPa was observed in Sr_2CoO_3F upon a gradual shrinkage of the Co-F bond length with pressure giving rise to a polyhedral transformation to the CoO_5F octahedron without a structural phase transition [64]. A complete HS to LS transition without going through IS was observed in SCRO and SCIO.

The inset of Fig. 7 presents integrated absolute difference (IAD) as a function of pressure [28,60–62] and the total IAD changes by about 0.07 from ambient pressure to 31 GPa. This value is half of that expected for a complete HS ($S = 2$) to LS ($S = 0$) transition found in SCRO [25] and SCIO [28]. The complete HS to LS transition in SCRO and SCIO requires high pressure up to 40 GPa, while at 14 GPa the LS state can be realized from an initial mixed spin state in LCRO. In order to distinguish between two scenarios of a possible Co^{3+} spin state in the LCRO, namely, a mixture of HS Co^{3+} and LS Co^{3+} or a pure IS Co^{3+} [32] to a LS state transition, we drew the difference spectra of Co-$K\beta$ emissions of LCRO obtained between ambient pressure (AP) and 14 GPa (dark yellow line) and that of SCRO between AP and 40 GPa (magenta) shown in Fig. 7 (below the x-ray emission spectra). The magenta line corresponds to the change in the spin number $\Delta S = 2$, while the dark yellow line describes the change in the spin number $\Delta S = 1$. These two difference spectra are almost identical apart from the scale factor of 2, giving rise to conclusion of the scenario of a nearly 1:1 mixture of HS Co^{3+} and LS Co^{3+} at the 300 K, AP condition in LCRO. Thus, the difference of the spectra does not show any sign for new features which would be expected for the presence of an intermediate spin state of Co^{3+} similar to SCRO and SCIO, since the IS state has a different line shape from the HS state as shown in the inset of Fig. 6 and in the previous experimental and the theoretical $K\beta$ spectra of Fe^{2+} ions with the same $3d^6$ configuration [65]. Therefore, a continuous spin-state transition from mixed HS-LS to LS under pressures in LCRO can be verified in agreement with the theoretical analysis on the Co-$L_{2,3}$ XAS spectra.

IV. CONCLUSION

We have observed a pure Co^{3+} and a pure Rh^{3+} valence state in the LCRO in the x-ray absorption spectroscopy. Comparing the experimental Co-$L_{2,3}$ XAS spectra of a LS Co^{3+} reference LCO and a HS Co^{3+} reference SCRO with those of LCRO, we have found that the Co-$L_{2,3}$ XAS spectrum of LCRO taken at room temperature is very similar to that of the 1:1 spectral weight ratio of LS:HS. Such situation was previously found in $LaCoO_3$ at 650 K. This experimental finding was further confirmed by our theoretical calculations; therefore we exclude the IS Co^{3+} with an octahedral coordination in $RCoO_3$. Furthermore, although IS states have the same spin number $S = 1$ as the 1:1 mixed HS ($S = 2$) and LS ($S = 0$) does, the spectral line shape and the intensity ratio between the Co-L_3 and the Co-L_2 edge of the calculated IS Co^{3+} states are very different between the two scenarios and can be easily distinguished from the experimental Co-$L_{2,3}$ XAS spectra. Therefore we safely rule out the IS Co^{3+} scenario. Under high pressure, the HS Co^{3+} is gradually converted to a complete LS at 14 GPa, which is much smaller than the pressure required for a complete HS to LS transition in Sr_2CoRuO_6 and $Sr_2Co_{0.5}Ir_{0.5}O_4$ observed previously.

ACKNOWLEDGMENTS

The research in Dresden was partially supported by the Deutsche Forschungs-gemeinschaft (DFG) through SFB 1143. NSRRC and Ministry of Science and Technology of Republic of China under Grant No. MOST 105-2113-M-213-005-MY3 supported this work. We acknowledge support from the Max Planck-POSTECH-Hsinchu Center for Complex Phase Materials.

[1] S. Sugano, Y. Tanabe, and H. Kamimura, *Multiplets of Transition-Metal Ions in Crystals* (Academic, New York, 1970), Chap. 5, Figs. 5 and 6.
[2] J. B. Goodenough, Prog. Solid State Chem. **5**, 333 (1971).
[3] J. B. Goodenough, Mater. Res. Bull. **6**, 967 (1971).
[4] M. W. Haverkort, Z. Hu, J. C. Cezar, T. Burnus, H. Hartmann, M. Reuther, C. Zobel, T. Lorenz, A. Tanaka, N. B. Brookes *et al.*, Phys. Rev. Lett. **97**176405 (2006).
[5] T. Negas and R. S. Roth, in *Proceedings of the 5th Materials Research Symposium on Solid State Chemistry*, National Bureau of Standards Special Publication No. 364, edited by R. S. Roth and S. J. Schneider, Jr. (U.S. Department of Commerce, Washington, DC, 1972), p. 233.
[6] H. Taguchi, Y. Takeda, F. Kanamaru, M. Shimada, and M. Koizumi, Acta Crystallogr., Sect. B **33**, 1298 (1977).

[7] R. H. Potze, G. A. Sawatzky, and M. Abbate, Phys. Rev. B **51**, 11501 (1995).

[8] P. M. Raccah and J. B. Goodenough, Phys. Rev. **155**, 932 (1967).

[9] C. Martin, A. Maignan, D. Pelloquin, N. Nguyen, and B. Raveau, Appl. Phys. Lett. **71**, 1421 (1997).

[10] M. Imada, A. Fujimori, and Y. Tokura, Rev. Mod. Phys. **70**, 1039 (1998).

[11] K. Takada, H. Sakurai, E. Takayama-Muromachi, F. Izumi, R. A. Dilanian, and T. Sasaki, Nature **422**, 53 (2003).

[12] J. Pérez, J. García, J. Blasco, and J. Stankiewicz, Phys. Rev. Lett. **80**, 2401 (1998).

[13] I. Terasaki, Y. Sasago, and K. Uchinokura, Phys. Rev. B **56**, R12685 (1997).

[14] J. Suntivich, K. J. May, H. A. Gasteiger, J. B. Goodenough, and Y. Shao-Horn, Science **334**, 1383 (2011).

[15] J. Hwang, R. R. Rao, L. Giordano, Y. Katayama, Y. Yu, and Y. Shao-Horn, Science **358**, 751 (2017).

[16] R. Heikes, R. Miller, and R. Mazelsky, Physica (Amsterdam) **30**, 1600 (1964).

[17] G. Blasse, J. Appl. Phys. **36**, 879 (1965).

[18] C. S. Naiman, R. Gilmore, B. DiBartolo, A. Linz, and R. Santoro, J. Appl. Phys. **36**, 1044 (1965).

[19] Y. Shimizu, T. Takahashi, S. Yamada, A. Shimokata, T. Jin-no, and M. Itoh, Phys. Rev. Lett. **119**, 267203 (2017).

[20] Y. Yokoyama, Y. Yamasaki, M. Taguchi, Y. Hirata, K. Takubo, J. Miyawaki, Y. Harada, D. Asakura, J. Fujioka, M. Nakamura *et al.*, Phys. Rev. Lett. **120**, 206402 (2018).

[21] R.-P. Wang, A. Hariki, A. Sotnikov, F. Frati, J. Okamoto, H.-Y. Huang, A. Singh, D.-J. Huang, K. Tomiyasu, C.-H. Du *et al.*, Phys. Rev. B **98**, 035149 (2018).

[22] G. E. Sterbinsky, R. Nanguneri, J. X. Ma, J. Shi, E. Karapetrova, J. C. Woicik, H. Park, J. W. Kim, and P. J. Ryan, Phys. Rev. Lett. **120**, 197201 (2018).

[23] K. I. Kobayashi, T. Kimura, H. Sawada, K. Terakura, and Y. Tokura, Nature **395**, 677 (1998).

[24] A. Kolchinskaya, P. Komissinskiy, M. B. Yazdi, M. Vafaee, D. Mikhailova, N. Narayanan, H. Ehrenberg, F. Wilhelm, A. Rogalev, and L. Alff, Phys. Rev. B **85**, 224422 (2012).

[25] J.-M. Chen, Y.-Y. Chin, M. Valldor, Z. Hu, J.-M. Lee, S.-C. Haw, N. Hiraoka, H. Ishii, C.-W. Pao, K.-D. Tsuei *et al.*, J. Am. Chem. Soc. **136**, 1514 (2014).

[26] S. Agrestini, C. Y. Kuo, D. Mikhailova, K. Chen, P. Ohresser, T. W. Pi, H. Guo, A. C. Komarek, A. Tanaka, Z. Hu *et al.*, Phys. Rev. B **95**, 245131 (2017).

[27] S. Agrestini, C. Y. Kuo, K. Chen, Y. Utsumi, D. Mikhailova, A. Rogalev, F. Wilhelm, T. Förster, A. Matsumoto, T. Takayama *et al.*, Phys. Rev. B **97**, 214436 (2018).

[28] Y.-Y. Chin, H.-J. Lin, Z. Hu, C.-Y. Kuo, D. Mikhailova, J.-M. Lee, S.-C. Haw, S.-A. Chen, W. Schnelle, H. Ishii *et al.*, Sci. Rep. **7**, 3656 (2017).

[29] T. Burnus, Z. Hu, H. Wu, J. C. Cezar, S. Niitaka, H. Takagi, C. F. Chang, N. B. Brookes, H. J. Lin, L. Y. Jang *et al.*, Phys. Rev. B **77**, 205111 (2008).

[30] V. S. Sergey, V. G. Vladimir, and I. K. Daniel, J. Phys.: Condens. Matter **28**, 086005 (2016).

[31] J. Li, A. E. Smith, K.-S. Kwong, C. Powell, A. W. Sleight, and M. A. Subramanian, J. Solid State Chem. **183**, 1388 (2010).

[32] T. Sudayama, H. Nakao, Y. Yamasaki, Y. Murakami, S. Asai, R. Okazaki, Y. Yasui, and I. Terasaki, J. Phys. Soc. Jpn. **86**, 094701 (2017).

[33] K. Sato, A. Matsuo, K. Kindo, Y. Hara, K. Nakaoka, Y. Kobayashi, and K. Asai, J. Phys. Soc. Jpn. **83**, 114712 (2014).

[34] T. Ichiro, A. Shinichiro, T. Hiroki, O. Ryuji, Y. Yukio, I. Yuka, and M. Taro, J. Phys.: Condens. Matter **29**, 235802 (2017).

[35] S. Asai, R. Okazaki, I. Terasaki, Y. Yasui, W. Kobayashi, A. Nakao, K. Kobayashi, R. Kumai, H. Nakao, Y. Murakami *et al.*, J. Phys. Soc. Jpn. **82**, 114606 (2013).

[36] K. Knížek, J. Hejtmánek, M. Maryško, Z. Jirák, and J. Buršík, Phys. Rev. B **85**, 134401 (2012).

[37] S. Asai, N. Furuta, Y. Yasui, and I. Terasaki, J. Phys. Soc. Jpn. **80**, 104705 (2011).

[38] H. Guo, K. Manna, H. Luetkens, M. Hoelzel, and A. C. Komarek, Phys. Rev. B **94**, 205128 (2016).

[39] Y. Wang, Y. Sui, P. Ren, L. Wang, X. J. Wang, W. H. Su, and H. J. Fan, Inorg. Chem. **49**, 3216 (2010).

[40] R. D. Shannon, Acta Crystallogr., Sect. A **32**, 751 (1976).

[41] P. G. Radaelli and S. W. Cheong, Phys. Rev. B **66**, 094408 (2002).

[42] W. C. M. Gomes, D. M. A. Melo, P. M. Pimentel, E. P. Marinho, M. A. F. Melo, and R. S. Nasar, Chem. Phys. **490**, 67 (2017).

[43] V. V. Sikolenko, I. O. Troyanchuk, V. V. Efimov, E. A. Efimova, S. I. Tiutiunnikov, D. V. Karpinsky, S. Pascarelli, O. Zaharko, A. Ignatov, D. Aquilanti *et al.*, J. Phys.: Conf. Ser. **712**, 012118 (2016).

[44] Y. Jiang, F. Bridges, N. Sundaram, D. P. Belanger, I. E. Anderson, J. F. Mitchell, and H. Zheng, Phys. Rev. B **80**, 144423 (2009).

[45] D. Mikhailova, Z. Hu, C.-Y. Kuo, S. Oswald, K. M. Mogare, S. Agrestini, J.-F. Lee, C.-W. Pao, S.-A. Chen, J.-M. Lee *et al.*, Eur. J. Inorg. Chem. **2017**, 587 (2017).

[46] Z. W. Li, Y. Drees, C. Y. Kuo, H. Guo, A. Ricci, D. Lamago, O. Sobolev, U. Rütt, O. Gutowski, T. W. Pi *et al.*, Sci. Rep. **6**, 25117 (2016).

[47] T. Burnus, Z. Hu, H. H. Hsieh, V. L. J. Joly, P. A. Joy, M. W. Haverkort, H. Wu, A. Tanaka, H. J. Lin, C. T. Chen *et al.*, Phys. Rev. B **77**, 125124 (2008).

[48] M. Merz, P. Nagel, C. Pinta, A. Samartsev, H. v. Löhneysen, M. Wissinger, S. Uebe, A. Assmann, D. Fuchs, and S. Schuppler, Phys. Rev. B **82**, 174416 (2010).

[49] A. Tanaka and T. Jo, J. Phys. Soc. Jpn. **63**, 2788 (1994).

[50] M. Magnuson, S. M. Butorin, J. H. Guo, and J. Nordgren, Phys. Rev. B **65**, 205106 (2002).

[51] O. Keski-Rahkonen and M. O. Krause, At. Data Nucl. Data Tables **14**, 139 (1974).

[52] J. C. Fuggle and S. F. Alvarado, Phys. Rev. A **22**, 1615 (1980).

[53] H.-F. Roth, G. Meyer, Z. Hu, and G. Kaindl, Z. Anorg. Allg. Chem. **619**, 1369 (1993).

[54] K. Hirsch, V. Zamudio-Bayer, F. Ameseder, A. Langenberg, J. Rittmann, M. Vogel, T. Möller, B. v. Issendorff, and J. T. Lau, Phys. Rev. A **85**, 062501 (2012).

[55] M. A. Korotin, S. Y. Ezhov, I. V. Solovyev, V. I. Anisimov, D. I. Khomskii, and G. A. Sawatzky, Phys. Rev. B **54**, 5309 (1996).

[56] X. Ou, F. Fan, Z. Li, H. Wang, and H. Wu, Appl. Phys. Lett. **108**, 092402 (2016).

[57] K. Tomiyasu, J. Okamoto, H. Y. Huang, Z. Y. Chen, E. P. Sinaga, W. B. Wu, Y. Y. Chu, A. Singh, R. P. Wang, F. M. F. de Groot *et al.*, Phys. Rev. Lett. **119**, 196402 (2017).
[58] S. Shibasaki, I. Terasaki, E. Nishibori, H. Sawa, J. Lybeck, H. Yamauchi, and M. Karppinen, Phys. Rev. B **83**, 094405 (2011).
[59] Z. Hu, S. Bertram, and G. Kaindl, Phys. Rev. B **49**, 39 (1994).
[60] K. Tsutsumi, H. Nakamori, and K. Ichikawa, Phys. Rev. B **13**, 929 (1976).
[61] G. Vankó, J.-P. Rueff, A. Mattila, Z. Németh, and A. Shukla, Phys. Rev. B **73**, 024424 (2006).
[62] J. M. Chen, J. M. Lee, S. C. Haw, S. A. Chen, V. Hardy, F. Guillou, S. W. Chen, C. Y. Kuo, C. W. Pao, J. F. Lee *et al.*, Phys. Rev. B **90**, 035107 (2014).
[63] K. Oka, M. Azuma, W.-t. Chen, H. Yusa, A. A. Belik, E. Takayama-Muromachi, M. Mizumaki, N. Ishimatsu, N. Hiraoka, M. Tsujimoto *et al.*, J. Am. Chem. Soc. **132**, 9438 (2010).
[64] Y. Tsujimoto, S. Nakano, N. Ishimatsu, M. Mizumaki, N. Kawamura, T. Kawakami, Y. Matsushita, and K. Yamaura, Sci. Rep. **6**, 36253 (2016).
[65] N. Schuth, S. Mebs, D. Huwald, P. Wrzolek, M. Schwalbe, A. Hemschemeier, and M. Haumann, Proc. Natl. Acad. Sci. USA **114**, 8556 (2017).

Correction: A middle initial was missing in the name of the seventh author and has been fixed.